$Fe_3(BF)_3(CO)_8$ structures with face-semibridging fluoroborylene ligands and a bicapped tetrahedral Fe_3B_3 cluster isoelectronic with $Os_6(CO)_{18}$†

Liancai Xu,[a] Qian-shu Li,*[ab] Yaoming Xie,[c] R. Bruce King*[ac] and Henry F. Schaefer III[c]

Received (in Montpellier, France) 19th May 2010, Accepted 15th July 2010
DOI: 10.1039/c0nj00382d

The report (2009) of an unusual and unexpected $Fe_3(\mu_3\text{-}BF)_2(\mu\text{-}BF)(CO)_9$ structure, an isoelectronic fluoroborylene analogue of the long known $Fe_3(CO)_{12}$, makes of interest the structures of the unsaturated $Fe_3(BF)_3(CO)_8$ isoelectronic with $Fe_3(CO)_{11}$. In this connection, seven singlet and eight triplet structures are found for $Fe_3(BF)_3(CO)_8$ within 30 kcal/mol in energy of the global minimum. Natural bond orbital (NBO) analysis aids in the understanding of the electronic structure of these systems. None of the predicted structures has even a single terminal BF group. In the three lowest energy singlet $Fe_3(BF)_3(CO)_8$ structures two of the BF groups are face-semibridging ligands whereas the third BF group is a simple edge-bridging ligand. The face-semibridging BF groups in these structures are joined to the Fe_3 triangle with two short Fe–B bonds of ~2.0 Å and one long Fe–B bond of 2.4 Å. A fourth singlet $Fe_3(B_3F_3)(CO)_7(\eta^2\text{-}\mu\text{-}CO)$ structure, lying only ~7 kcal/mol above the lowest energy singlet structure, has a central Fe_3B_3 capped tetrahedron analogous to the central Os_6 bicapped tetrahedron in the long-known isoelectronic $Os_6(CO)_{18}$. This last cluster suggests the potential accessibility of fluoroborane metal carbonyl clusters having deltahedral structures related to those found in the deltahedral boranes.

1. Introduction

The fluoroborylene ligand, BF, is of interest since it is isoelectronic with the carbonyl ligand, CO, a foundational subunit of organometallic chemistry.[1] In this connection, metal carbonyl chemistry is highly developed, owing at least partially to the ready availability of carbon monoxide as a stable gas that can be used to introduce carbonyl groups into a variety of compounds. In contrast, the instability of BF (boron monofluoride)[2] has limited the development of an analogous chemistry of metal fluoroborylene complexes. Fragmentary reports of the fluoroborylene iron derivatives $Fe(BF)L_4$ (L = CO and PF_3),[3] have appeared in conference proceedings[4] but these compounds have not been properly characterized. The first fluoroborylene metal derivative that has been fully characterized is the ruthenium complex $Cp_2Ru_2(CO)_4(\mu\text{-}BF)$, which was synthesized only in 2009 and structurally characterized by X-ray diffraction.[5] Even more recently, terminal fluoroborylene complexes of the type FB = MF_2 (M = Ti, Zr, Hf, Th) were generated in low temperature matrices by reactions of laser ablated metal atoms with BF_3 and characterized by their comparison of their infrared spectra with those predicted by density functional theory.[6,7] In addition metal complexes with bridging non-fluorinated borylene ligands BX (X = H, CN, CR, OMe and OEt), have been studied extensively.[8–12]

The potential of metal fluoroborylene chemistry naturally leads to particular focus on metal carbonyl derivatives in which one or more of the CO groups have been replaced by BF groups. Initial work on the iron compounds of this type predicted a structure for $Fe(BF)(CO)_4$ analogous to $Fe(CO)_5$ as well as a triply bridged $Fe_2(\mu\text{-}BF)_2(\mu\text{-}CO)(CO)_6$ structure analogous to $Fe_2(CO)_9$ (= $Fe_2(\mu\text{-}CO)_3(CO)_6$).[13] Furthermore, BF ligands were found to be preferred over CO ligands as bridging groups. However, a big surprise came from the observation that the lowest energy structure for $Fe_3(BF)_3(CO)_9$ was neither a doubly bridged structure similar to $Fe_3(CO)_{12}$ nor an unbridged structure similar to $M_3(CO)_{12}$ (M = Ru, Os). Instead, a novel $Fe_3(\mu_3\text{-}BF)_2(\mu\text{-}BF)(CO)_9$ structure is found with a trigonal bipyramidal Fe_3B_2 core with the iron atoms in equatorial positions and the boron atoms in axial positions (Fig. 1).[14] The energy of this unusual $Fe_3(\mu_3\text{-}BF)_2(\mu\text{-}BF)(CO)_9$ structure was predicted to be ~19 kcal/mol below the next higher energy structure, indicating a highly favored structure. Furthermore, the observation of two face-bridging μ_3-BF groups in this lowest energy $Fe_3(BF)_3(CO)_9$ suggests that face-bridging is a particularly favorable coordination mode of the BF group. This aspect of the unusual $Fe_3(\mu_3\text{-}BF)_2(\mu\text{-}BF)(CO)_9$ structure is not entirely surprising, since face-bridging allows the fluoroborylene boron to have tetrahedral coordination with a formal B–F single bond (Fig. 2). The favorability of face-coordinated μ_3-BF groups suggests the use of BF ligands to stabilize metal triangles in

[a] *Center for Computational Quantum Chemistry, South China Normal University, Guangzhou 510631, P. R. China*
[b] *Institute of Chemical Physics, Beijing Institute of Technology, Beijing 100081, P. R. China*
[c] *Department of Chemistry and Center for Computational Chemistry, University of Georgia, Athens, Georgia 30602, USA*

† Electronic supplementary information (ESI) available: Tables S1–S3: Theoretical harmonic vibrational frequencies for $Fe_3(BF)_3(CO)_8$ (15 structures) from B3LYP/DZP; Tables S4–S18: Theoretical Cartesian coordinates for $Fe_3(BF)_3(CO)_8$ (15 structures), using the BP86/DZP method.; Table S19: Wiberg bond indices from NBO analysis for **8-1S**, **8-4S**, **9-1S** and $Fe(BF)(CO)_4$ with C_{2v} symmetry. Complete Gaussian 03 reference (ref. 44). See DOI: 10.1039/c0nj00382d

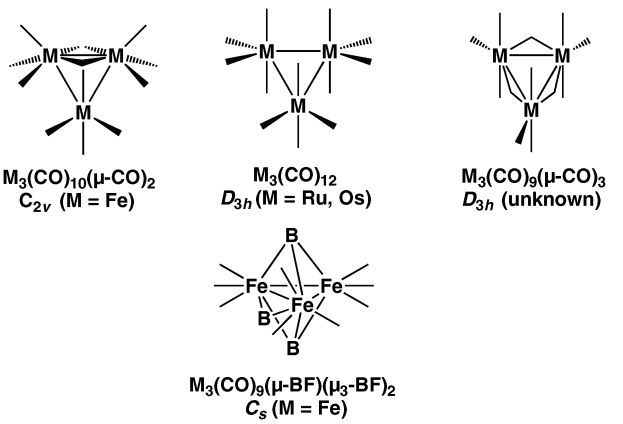

$M_3(CO)_{10}(\mu\text{-}CO)_2$ C_{2v} (M = Fe)

$M_3(CO)_{12}$ D_{3h} (M = Ru, Os)

$M_3(CO)_9(\mu\text{-}CO)_3$ D_{3h} (unknown)

$M_3(CO)_9(\mu\text{-}BF)(\mu_3\text{-}BF)_2$ C_s (M = Fe)

Fig. 1 A comparison of the $M_3(CO)_{12}$ structures with the lowest energy structure found for $Fe_3(BF)_3(CO)_9$ (carbonyl groups and fluorine atoms omitted for clarity).

trinuclear complexes including metal carbonyl derivatives. This might allow the synthesis of more highly unsaturated trinuclear metal carbonyl complexes without breaking the metal–metal bonds in the underlying triangular M_3 framework. In this connection, some trinuclear metal complexes containing non-fluorinated borylene ligands bridging a metal triangle have been synthesized including $\{(\eta^5\text{-}C_5Me_5)Ru\}_3(\mu\text{-}H)_3(\mu_3\text{-}BX)\}$ (X = OMe, OEt)[10] and $[(\mu^3\text{-}Bu^tB)\{[(\eta^5\text{-}C_5H_4Me)Mn(CO)_2][Pd\text{-}(PCy_3)]_2\}]$.[11]

This paper describes a theoretical study of $Fe_3(BF)_3(CO)_8$. This system was chosen for the following reasons: (1) It is one of the simplest possible unsaturated trinuclear fluoroborylene metal carbonyls; (2) It can be derived from the previously studied[14] $Fe_3(BF)_3(CO)_9$ by removal of a carbonyl group, therefore allowing an assessment of the structural changes occurring upon introducing unsaturation; (3) The isoelectronic unsaturated homoleptic trinuclear iron carbonyl $Fe_3(CO)_{11}$ has already been studied;[15] (4) Extensive known iron carbonyl chemistry provides a number of possible synthetic approaches, making this a plausible synthetic target, particularly if $Fe(BF)(CO)_4$ or $Fe_3(BF)_3(CO)_9$ become available. An unanticipated result from this theoretical study is the discovery of a low-energy $Fe_3(B_3F_3)(CO)_7(\eta^2\text{-}\mu\text{-}CO)$ structure with a four-electron donor bridging carbonyl group and a central Fe_3B_3 bicapped tetrahedron analogous to the central Os_6 bicapped tetrahedron in the long-known[16] $Os_6(CO)_{18}$.

Theoretical methods

Electron correlation effects were considered using density functional theory (DFT) methods, which have evolved as a practical and effective computational tool, especially for organometallic compounds.[17–31] Two DFT methods were used in this study. The popular B3LYP method combines the three-parameter Becke exchange functional (B3) with the Lee–Yang–Parr (LYP) generalized gradient correlation functional.[32,33] The BP86 method combines Becke's 1988 exchange functional (B) with Perdew's 1986 gradient corrected correlation functional (P86).[34,35] The BP86 method has been found to be somewhat more reliable than B3LYP for the type of organometallic systems considered here, especially for the prediction of vibrational frequencies.[36–38]

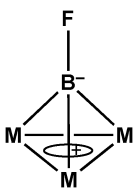

Fig. 2 Schematic representation of a μ_3-BF ligand bridging a metal triangle, showing the formal negative charge on the boron atom and the formal positive charge on the metal triangle.

For comparison with our previous research, the same double-ζ plus polarization (DZP) basis sets were adopted in this research. Thus one set of pure spherical harmonic d functions with orbital exponents $\alpha_d(B) = 0.7$, $\alpha_d(C) = 0.75$, $\alpha_d(O) = 0.85$, and $\alpha_d(F) = 1.0$ for boron, carbon, oxygen, and fluorine, respectively, was added to the standard Huzinaga-Dunning contracted DZ sets,[39–41] designated as (9s5p1d/4s2p1d). The loosely contracted DZP basis set for iron is the Wachters primitive set[42] augmented by two sets of p functions and one set of d functions, contracted following Hood, Pitzer and Schaefer,[43] designated as (14s11p6d/10s8p3d).

The geometries of all structures were fully optimized using both DFT methods. Harmonic vibrational frequencies were determined by evaluating analytically the second derivatives of the energy with respect to the nuclear coordinates. All calculations were performed with the Gaussian 03 program package.[44] The fine grid (75, 302) was the default for the numerical evaluation of the integrals, while the finer grid (120, 974) was used to evaluate the small imaginary vibrational frequencies. All of the predicted triplet structures in this research are found to have negligible spin contamination, with the $\langle S^2\rangle = S(S+1)$ values close to the ideal outcome of 2.0.

A given $Fe_3(BF)_3(CO)_a$ structure is designated as **a-bA** where **a** is the number of CO groups, and **b** orders the structures according to their relative energies based on the BP86 method. **A** indicates whether the structure is a singlet (**S**) or triplet (**T**). Thus the lowest lying singlet $Fe_3(BF)_3(CO)_8$ structure is designated **8-1S**.

3. Results

3.1 Molecular structures

Seven singlet and eight triplet structures are found for $Fe_3(BF)_3(CO)_8$ within ~30 kcal/mol, suggesting a very complicated potential energy surface for $Fe_3(BF)_3(CO)_8$ (Fig. 3 and 4 and Table 1). All three BF groups in all 15 structures are bridging ligands of some type; no $Fe_3(BF)_3(CO)_8$ structures with even a single terminal BF group were found. The global minimum for $Fe_3(BF)_3(CO)_8$ depends on the method used. Thus B3LYP predicts **8-2T** to be the global minimum at 1.8 kcal/mol below **8-1S**. However, BP86 predicts **8-1S** to lie 6.8 kcal/mol below **8-2T**. This is consistent with the tendency for B3LYP to favor triplet states relative to BP86 discussed by Reiher, Salomon, and Hess.[45] Thus B3LYP is a hybrid functional while BP86 is a pure functional; triplet states are found to be stabilized for hybrid exchange correlation functionals relative to pure functionals. Unless otherwise

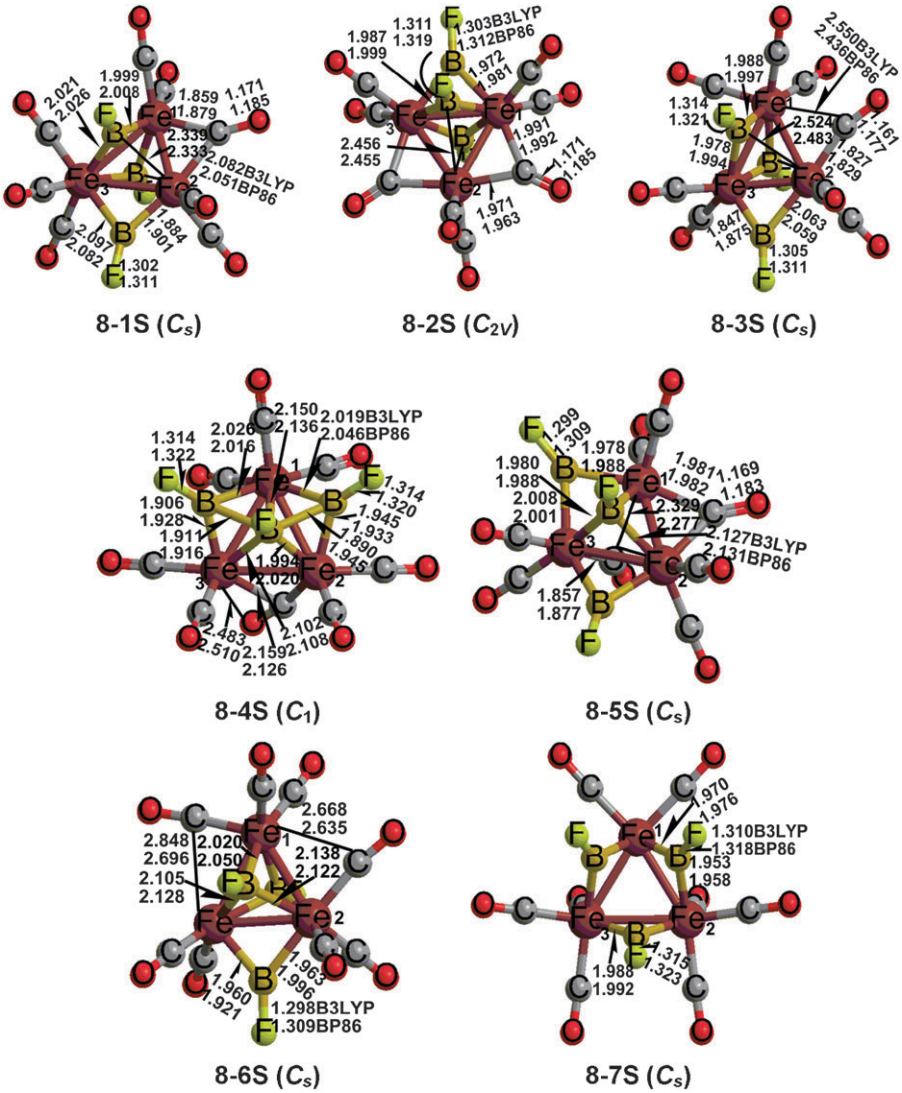

Fig. 3 Seven optimized singlet structures for $Fe_3(BF)_3(CO)_8$.

indicated, all $Fe_3(BF)_3(CO)_8$ structures are genuine minima with no imaginary vibrational frequencies.

The $Fe_3(BF)_3(CO)_8$ structure **8-1S** with C_s symmetry has four bridges, namely three bridging BF groups and one bridging CO group, and is predicted to be a genuine minimum by both the B3LYP and BP86 methods (Fig. 3 and Table 1). Two BF groups bridge an edge of the Fe_3 triangle with Fe–B distances of 2.01 Å. In addition, these boron atoms are more weakly bonded to the third iron atom with longer Fe–B distances of 2.339 Å (B3LYP) or 2.333 Å (BP86). Such BF groups can be considered to be face-semibridging BF groups. The two lowest ν(BF) frequencies in **8-1S**, namely 1323 and 1308 cm^{-1} (Table 2) can be assigned to these face semibridging BF groups. The iron-iron distances in **8-1S** are 2.280 Å, 2.704 Å, and 2.650 Å (B3LYP) or 2.276 Å, 2.697 Å, and 2.627 Å (BP86). These bond distances suggest one double Fe═Fe bond and two single Fe–Fe bonds, thereby providing each iron atom with the favored 18-electron configuration. The $Fe_3(BF)_3(CO)_8$ structure **8-1S** can be obtained *via* removing a terminal carbonyl group from the lowest energy $Fe_3(BF)_3(CO)_9$ structure (Fig. 1). One of the remaining carbonyl groups then becomes a bridging carbonyl group and the two face-bridging μ_3-BF groups move away from the iron atom bearing two edge-bridging groups (μ-BF + μ-CO) to become face-semibridging BF groups. The short Fe═Fe edge, assigned to the formal double bond, is the one bridged by the carbonyl group.

The next low lying C_{2v} singlet $Fe_3(BF)_3(CO)_8$ structure **8-2S**, at 5.6 kcal/mol (B3LYP) or 1.4 kcal/mol (BP86) above **8-1S**, is an unusual structure with five bridging groups across the three edges of an isosceles Fe_3 triangle (Fig. 3 and Table 1). The unique edge of the isosceles triangle in **8-2S** is bridged by all three BF groups, whereas each of the other two edges is bridged by a single carbonyl group. The top and the bottom edge-bridging BF groups relative to the plane of the Fe_3 triangle form a weak bond to the third iron atom with Fe–B distances of 2.546 Å (B3LYP) or 2.445 Å (BP86) so that they become face-semibridging BF groups. The Fe–Fe distances in **8-2S** are 2.468 Å (two edges) and 2.533 Å (B3LYP) or 2.448 Å (two edges) and 2.545 Å (BP86). In this case, differentiation between formal single and double bonds by edge-lengths is not clear.

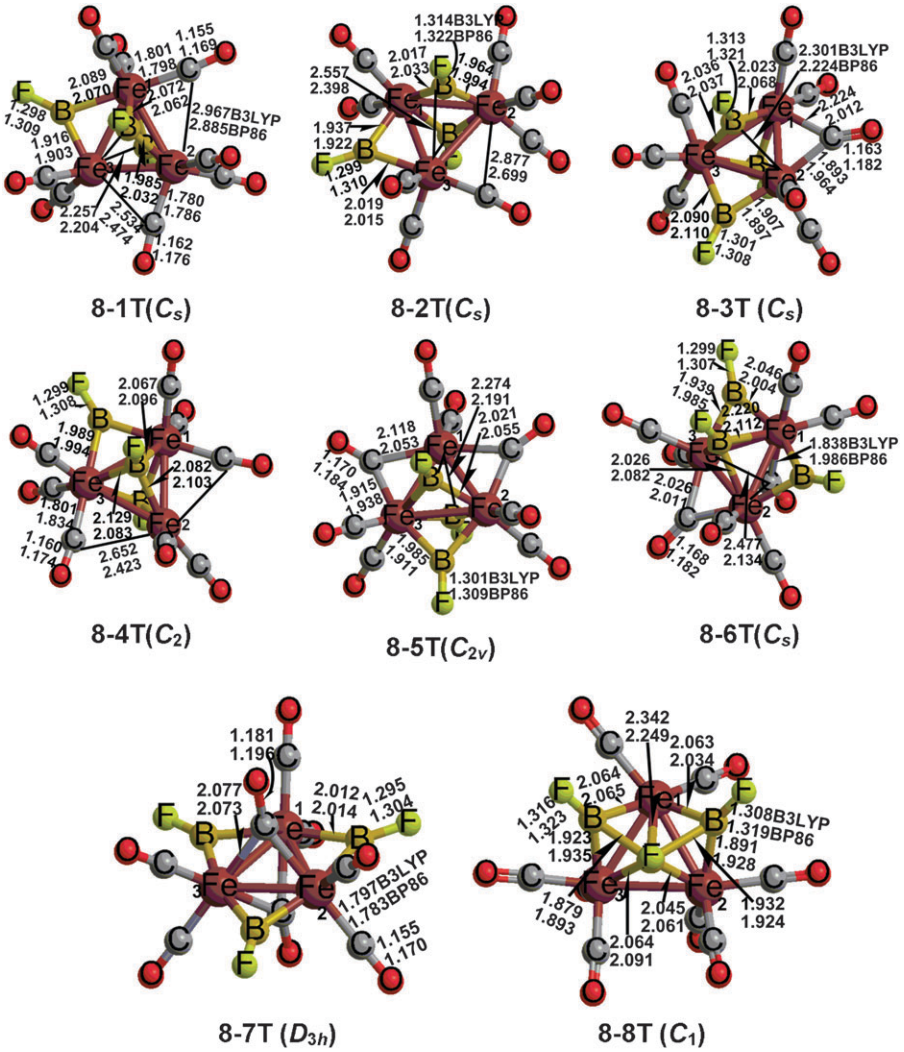

Fig. 4 Eight optimized triplet structures for $Fe_3(BF)_3(CO)_8$.

The next singlet $Fe_3(BF)_3(CO)_8$ structure, namely **8-3S**, has three bridging BF groups and one semibridging CO group, and lies 1.5 kcal/mol (B3LYP) or 4.0 kcal/mol (BP86) in energy above **8-1S** (Fig. 3 and Table 1). Analogous to **8-2S**, structure **8-3S** also has two face-semibridging BF groups bridging one Fe–Fe edge and weakly bonded to the third iron

Table 1 Total energies (E, in Hartree), relative energies (ΔE, in kcal/mol), numbers of imaginary vibrational frequencies (Nimag), and Fe–Fe distances for the 15 $Fe_3(BF)_3(CO)_8$ structures

	B3LYP						BP86					
	$-E$	ΔE	Nimag	$R_{Fe1-Fe2}$	$R_{Fe1-Fe3}$	$R_{Fe2-Fe3}$	$-E$	ΔE	Nimag	$R_{Fe1-Fe2}$	$R_{Fe1-Fe3}$	$R_{Fe2-Fe3}$
8-1S(C_s)	5072.56353	0.0	0	2.280	2.704	2.650	5073.30536	0.0	0	2.276	2.697	2.627
8-2S(C_{2v})	5072.55462	5.6	0	2.468	2.533	2.468	5073.30313	1.4	0	2.448	2.545	2.448
8-3S(C_s)	5072.56113	1.5	0	2.716	2.610	2.387	5073.29899	4.0	0	2.649	2.610	2.364
8-4S(C_1)	5072.55090	7.9	0	2.706	2.722	2.484	5073.29761	4.9	0	2.681	2.703	2.472
8-5S(C_s)	5072.53878	15.6	49*i*	2.347	2.562	2.562	5073.28807	10.8	24*i*	2.344	2.552	2.552
8-6S(C_s)	5072.53423	18.4	59*i*	2.565	2.579	2.540	5073.28114	15.2	40*i*	2.519	2.557	2.532
8-7S(C_s)	5072.53646	17.0	10*i*	2.559	2.559	2.696	5073.28021	15.8	4*i*	2.536	2.536	2.687
8-1T(C_s)	5072.56266	0.5	0	2.667	2.609	2.449	5073.29449	6.8	0	2.624	2.582	2.402
8-2T(C_s)	5072.56632	–1.8	0	2.568	2.519	2.725	5073.29335	7.5	0	2.553	2.448	2.606
8-3T(C_s)	5072.56440	–0.5	0	2.380	2.635	2.636	5073.29098	9.0	0	2.354	2.622	2.590
8-4T(C_2)	5072.55852	3.1	14*i*	2.623	2.592	2.623	5073.28497	12.8	103*i*	2.499	2.583	2.499
8-5T(C_{2v})	5072.54871	9.3	225*i*	2.465	2.465	2.571	5073.28418	13.3	185*i*,15*i*	2.424	2.424	2.569
8-6T(C_s)	5072.53294	19.2	0	2.524	2.524	2.515	5073.27395	19.7	0	2.479	2.479	2.460
8-7T(D_{3h})	5072.51200	32.3	64*i*	2.482	2.482	2.482	5073.25438	32.0	0	2.472	2.472	2.472
8-8T(C_1)	5072.52081	26.8	0	2.629	2.615	2.683	5073.25131	33.9	0	2.559	2.550	2.629

Table 2 The ν(CO) and ν(BF) stretching vibrational frequencies (cm^{-1}) and infrared intensities in km/mol (in parentheses) for the trinuclear $Fe_3(BF)_3(CO)_8$ derivatives predicted by the BP86 method. The bridging ν(CO) and ν(BF) frequencies are in **bold face**

	ν(CO)	ν(BF)
8-1S(C_s)	2057(164),2020(1389),2012(1928),2004(977), 2002(23),1987(783),1982 (121),**1902(580)**	**1355(433),1323(23),1308(594)**
8-2S(C_{2v})	2054(8),2022(1367),2014(1958), 2003(1681) 1998(0),1992(141),**1904(209),1884 (806)**	**1350(432),1338(136),1318(594)**
8-3S(C_s)	2059(176),2025(1485),2007(1978),2006(934) 1997(50), 1991(542), 1977(383),1939(279)	**1371(499),1325(10),1308(584)**
8-4S(C_1)	2055(35),2024(1708),2016(2000),2002(1085), 1993(234),1987(41), 1977(20),**1847(313)**	**1333(483),1318(381),1191(196)**
8-5S(C_s)	2051(2) 2018(1472) 2016(1758) 2002(1062) 1994(661) 1990(4) **1906(608) 1847(245)**	**1363(358),1346(727),1312(254)**
8-6S(C_s)	2050(201),2012(1416),1999(1300),1993(2024) 1992(297),1979(1),1963(513),1958(232)	**1367(426),1287(17), 1262 (465)**
8-7S(C_s)	2047(89),2010(2158),2009(1810),1988(17) 1981(417),1980(945),1971(100),1950(0)	**1350(741),1314(102),1296(222)**
8-1T(C_s)	2054(213),2012(1400),2002(1813),1999(1290), 1992(220) 1988(496),1973(529),1950(335)	**1357 (457),1305(15),1294(540)**
8-2T(C_s)	2054(174.0),2013(1534),2003(968),2000(2297) 1988 (75),1984(999),1979(64),1968(72)	**1359(459),1318(11) 1296(501)**
8-3T(C_s)	2052(78),2014(1499),2003(2084),2001(1203) 1991(46),1990(578),1984(287),**1892(480)**	**1368(480),1314(8),1295(520)**
8-4T(C_2)	2051(21), 2015(1518), 2000(1477), 2000(2052), 1994(247),1976(502),1958(447),1952(6)	**1363(487),1312(7),1303(629)**
8-5T(C_{2v})	2048(2), 2012(1625), 2010(1881),1998(1301), 1993(0),1981(718),**1907(219),1892(812)**	**1354(509) 1334 (49) 1325(598)**
8-6T(C_s)	2044(7),2008(1662),2005(1794),1995(1797), 1989(48),1987(41),**1907(499),1803(245)**	**1374(367),1355(790),1331(251)**
8-7T(D_{3h})	2040(0),2008(1593),2008(1594),1995(1796) 1989(0),1989(0),**1797(0),1776(473)**	**1393(0),1362(830),1362(830)**
8-8T(C_1)	2056(302),2014(1796), 2008(2027), 1985(551),1996(722),1983(309),1972(23),1969(112)	**1342(602),1321(294),1157(219)**

atom with the long Fe–B distances of 2.524 Å (B3LYP) or 2.483 Å (BP86). The third BF group in **8-3S**, however, bridges a different edge. The Fe–Fe distances in **8-3S** of 2.716 Å, 2.610 Å, and 2.378 Å (B3LYP) or 2.649 Å, 2.610 Å, and 2.364 Å (BP86) correspond to two Fe–Fe single bonds and one Fe = Fe double bond, thereby giving each of the three iron atoms the favored 18-electron configuration. Structure **8-3S** differs from **8-1S** by the distribution of the carbonyl groups.

An unusual singlet $Fe_3(BF)_3(CO)_8$ structure **8-4S** was found in which the three BF groups are linked to form a B_3F_3 chain (Fig. 3 and Table 1). Furthermore, the central Fe_3B_3 unit forms a bicapped tetrahedron with Fe1 and the central boron atom at the degree 5 vertices, the remaining two iron atoms at the degree 4 vertices, and the remaining two boron atoms at the degree 3 vertices. This bicapped tetrahedron is similar to the Os_6 bicapped tetrahedron found in $Os_6(CO)_{18}$, which has been structurally characterized by X-ray crystallography.[16] Structure **8-4S** is predicted to lie 7.9 kcal/mol (B3LYP) or 4.9 kcal/mol (BP86) above **8-1S** in energy. The B–B distances between the central and outer boron atoms in **8-4S** are 1.911 Å and 1.890 Å (B3LYP) or 1.916 Å or 1.945 Å (BP86). The central BF group in the B_3F_3 chain of **8-4S** exhibits a very low ν(BF) frequency of 1193 cm^{-1} compared with the 1333 and 1318 cm^{-1} ν(BF) frequencies of the two outer BF groups. The Fe3–O distance of 2.483 Å (B3LYP) or 2.510 Å (BP86) in **8-4S** indicates that the bridging CO group is a four-electron donor η^2-μ-CO group, which is consistent with its low ν(CO) frequency of 1847 cm^{-1}. The unbridged Fe–Fe distances in **8-4S** of 2.706 Å and 2.722 Å (B3LYP) or 2.681 Å and 2.703 Å (BP86) are similar to the experimental[46] unbridged Fe–Fe distance of 2.68 Å for $Fe_3(CO)_{12}$. The Fe–Fe distance bridged by the η^2-μ-CO group in **8-4S** of 2.484 Å (B3LYP) or 2.472 Å (BP86) can be compared with the experimental[46] doubly bridged Fe–Fe distance of 2.56 Å in $Fe_3(CO)_{12}$. All of the Fe–Fe bonds in **8-4S** can be considered to be formal single bonds, thereby giving each iron atom the favored 18-electron configuration in this trinuclear structure with a four-electron donor bridging η^2-μ-CO group.

The remaining three singlet $Fe_3(BF)_3(CO)_8$ structures lie at significantly higher energies than the first three singlet structures. Thus the C_s singlet $Fe_3(BF)_3(CO)_8$ structure **8-5S** with five bridges, including three bridging BF groups, one bridging CO group and one semi-bridging CO group, is predicted to lie 15.6 kcal/mol (B3LYP) or 10.8 kcal/mol (BP86) in energy above **8-1S**. Structure **8-5S** has one small imaginary frequency at 49*i* cm^{-1} (B3LYP) or 24*i* cm^{-1} (BP86). By following the corresponding normal mode with the B3LYP method structure **8-5S** collapses to **8-1S**. However, following the corresponding normal mode with the BP86 method leads to only a slight change in energy and geometry. The B–B distance in **8-5S** is 2.447 Å (B3LYP) or 2.392 Å (BP86), which is too long for a direct bond. Two of the three Fe–Fe distances in **8-5S** are 2.562 Å (B3LYP) or 2.552 Å (BP86), whereas the third Fe–Fe distance is 2.347 Å (B3LYP) or 2.344 Å (BP86). The first two Fe–Fe distances correspond to formal single bonds and the third significantly shorter Fe=Fe distance to a formal double bond. This gives all three iron atoms in **8-5S** the favored 18-electron configurations.

The next singlet $Fe_3(BF)_3(CO)_8$ structure **8-6S**, with three bridging BF groups, one bridging CO group, and one

semibridging CO group, lies 18.4 kcal/mol (B3LYP) or 15.2 kcal/mol (BP86) above **8-1S**. Structure **8-6S** is not a genuine minimum but has a small imaginary frequency at $59i$ cm^{-1} (B3LYP) or $40i$ cm^{-1} (BP86). Following the corresponding normal mode of **8-6S** leads to **8-1S**.

The last singlet $Fe_3(BF)_3(CO)_8$ structure **8-7S** is of a different type, with all terminal CO groups and a BF group bridging each edge of the Fe_3 triangle. Structure **8-7S** lies 17.0 kcal/mol (B3LYP) or 15.8 kcal/mol (BP86) in energy above **8-1S** and has a negligible imaginary frequency at $10i$ cm^{-1} (B3LYP) or $4i$ cm^{-1} (BP86).

The C_s triplet $Fe_3(BF)_3(CO)_8$ structure **8-1T** with two face-bridging BF groups, one edge-bridging BF group, and one semibridging CO group lies 0.5 kcal/mol (B3LYP) or 6.8 kcal/mol (BP86) above **8-1S** (Fig. 4 and Table 1). The face-bridging BF groups in **8-1T** exhibit relatively low ν(BF) frequencies (BP86) at 1305 and 1294 cm^{-1} (Table 2). The Fe–Fe distances in **8-1T** are 2.667 Å, 2.609 Å, and 2.449 Å (B3LYP) or 2.624 Å, 2.582 Å, and 2.402 Å (BP86). The short Fe–Fe edge is the one bridged by the semibridging CO group. After considering the expected edge-shortening by this semi-bridging CO group, all three Fe–Fe edges can be considered to be formal single bonds. This gives one iron atom the favored 18-electron configuration and the other two iron atoms 17-electron configurations, consistent with a trinuclear triplet state structure.

The second triplet $Fe_3(BF)_3(CO)_8$ structure **8-2T** is the global minimum by B3LYP and lies 7.5 kcal/mol (BP86) above the global minimum **8-1S** by B3LYP (Fig. 4 and Table 1). Structure **8-2T** is similar to **8-1S** except that the bridging CO group in **8-1S** becomes a semibridging CO group in **8-2T**. In **8-2T** the two face-semibridging BF groups have short Fe–B distances of 1.964 Å and 2.017 Å (B3LYP) or 1.994 Å and 2.033 Å (BP86) and long Fe–B distances of 2.557 Å (B3LYP) or 2.398 Å (BP86). The Fe–Fe distances in **8-2T** bridged by one or two μ-BF groups are 2.519 Å and 2.568 Å (B3LYP) or 2.448 Å and 2.553 Å (BP86) as compared with the experimental[46] 2.56 Å doubly bridged Fe–Fe distance in $Fe_3(CO)_{12}$. Similarly, the unbridged Fe2–Fe3 distance in **8-2T** of 2.725 Å (B3LYP) or 2.606 Å (BP86) is similar to the experimental[46] 2.68 Å unbridged Fe–Fe distance in $Fe_3(CO)_{12}$. The similarity of the Fe–Fe distances in **8-2T** to those in $Fe_3(CO)_{12}$ suggests formal single bonds. This gives one iron atom the favored 18-electron configuration and the other two iron atoms 17-electron configurations, consistent with a trinuclear triplet.

The triplet $Fe_3(BF)_3(CO)_8$ structure **8-5T** with three bridging BF groups and two bridging CO groups is predicted to lie 9.3 kcal/mol (B3LYP) or 13.3 kcal/mol (BP86) above **8-1S** (Fig. 4 and Table 1). However, **8-5T** is not a genuine minimum but has a significant imaginary vibrational frequency of $225i$ cm^{-1} (B3LYP) or $185i$ and $15i$ cm^{-1} (BP86). Following the normal mode corresponding to this large imaginary vibrational frequency leads to **8-4T** with a decrease in symmetry from C_{2v} in **8-5T** to C_2 in **8-4T**. Structure **8-4T** lies 3.1 kcal/mol (B3LYP) or 12.8 kcal/mol (BP86) in energy above **8-1S** and has a negligible imaginary vibrational frequency at $14i$ cm^{-1} by B3LYP but a significant imaginary vibrational frequency at $103i$ cm^{-1} by BP86. Following the normal mode of the imaginary vibrational frequency at $103i$ cm^{-1} leads from structure **8-4T** to **8-3T**. Structure **8-4T** has two face-bridging μ_3-BF groups and two semibridging CO groups. For the latter the short M–C distances are 1.801 Å (B3LYP) or 1.834 Å (BP86) and the long M–C distances are 2.652 Å (B3LYP) or 2.423 Å (BP86). The Fe–Fe distances in **8-4T** are 2.592 Å, 2.623 Å, and 2.623 Å, corresponding to three formal single bonds, giving one iron the favored 18-electron configuration and the other two iron atoms 17-electron configurations for a trinuclear triplet.

The triplet $Fe_3(BF)_3(CO)_8$ structure **8-3T** is similar to **8-1S** with two face-semibridging BF groups, one edge-bridging BF group, and one bridging CO group (Fig. 4 and Table 1). Structure **8-3S** lies 0.5 kcal/mol below **8-1S** using B3LYP but 9.0 kcal/mol above **8-1S** using BP86. The long Fe–B distances from the face-semibridging BF groups in **8-3T** are 2.301 Å (B3LYP) or 2.224 Å (BP86). The Fe–Fe distances in **8-3T** are 2.380 Å, 2.635 Å, and 2.636 Å (B3LYP) or 2.354 Å, 2.622 Å, and 2.590 Å (BP86). The shortest Fe–Fe distance in **8-3T** is bridged by a CO group and is longer by $\sim$0.1 Å than the similar CO-bridged Fe–Fe edge in structure **8-1S**. For this reason all of the Fe–Fe bonds in **8-3T** are interpreted as formal single bonds, thereby giving two iron atoms 17-electron configurations and the third iron atom an 18-electron configuration for a trinuclear triplet.

The C_s triplet $Fe_3(BF)_3(CO)_8$ structure **8-6T**, at 19.2 kcal/mol (B3LYP) or 19.7 kcal/mol (B3LYP) above **8-1S**, has five bridging groups including three BF groups and two CO groups (Fig. 4 and Table 1). Structure **8-6T** is analogous to **8-5S**, except that the shortest Fe–Fe distance in **8-6T** of 2.515 Å (B3LYP) or 2.460 Å (BP86) is significantly longer than the shortest distance of 2.347 Å (B3LYP) or 2.344 Å (BP86) in **8-5S**. This suggests that all of the Fe–Fe bonds in **8-6T** are formal single bonds. This gives one iron the favored 18-electron configuration but the other two iron atoms 17-electron configurations, corresponding to a trinuclear triplet.

The only triplet $Fe_3(BF)_3(CO)_8$ structure with D_{3h} symmetry, namely **8-7T**, has three BF groups bridging each edge of the Fe_3 triangle and two μ_3-CO groups bridging all three iron atoms. (Fig. 4 and Table 1) However, structure **8-7T** is a relatively high energy structure, lying 32.3 kcal/mol (BP86) or 32.0 kcal/mol (B3LYP) above **8-1S**. Structure **8-7T** is derived from **8-5T** by swapping the position of the two apical bridging μ_3-BF groups with two equatorial edge-bridging μ-CO groups. The two μ_3-CO groups exhibit unusually low ν(CO) frequencies (Table 2) of 1797 and 1776 cm^{-1} (BP86). The Fe–Fe distances in **8-7T** are 2.482 Å (B3LYP) or 2.472 Å (BP86). These correspond to formal single bonds, which are shortened by the two μ_3-CO groups. This gives one iron the favored 18-electron configuration and the other two iron atoms 17-electron configurations consistent with a trinuclear triplet.

The C_1 triplet $Fe_3(BF)_3(CO)_8$ structure **8-8T**, lying at the at the relatively high energy of 26.8 kcal/mol (B3LYP) or 33.9 kcal/mol (BP86) above **8-1S**, has all terminal CO groups and three bridging BF groups (Fig. 4 and Table 1). The triplet $Fe_3(BF)_3(CO)_8$ structure **8-8T** is very similar to the singlet structure **8-4S** (Fig. 3 and Table 1) with the three BF groups forming a B_3 chain and an underlying Fe_3B_3 bicapped

tetrahedron. The major difference between **8-8T** and **8-4S** is that **8-4S** has one four-electron donor bridging η^2-μ-CO group whereas all of the carbonyl groups in **8-8T** are terminal carbonyl groups.

3.2 Atomic population and natural bond orbital (NBO) analyses

Table 3 lists the natural charges[47] on the iron, boron and fluorine atoms for the fluoroborylene derivatives $Fe(BF)(CO)_4$,[13] $Fe_3(\mu_3\text{-}BF)_2(\mu\text{-}BF)(CO)_9$ (structure **9-1S** in ref. 14), $Fe_3(\mu\text{-}BF)_3(CO)_8$ (structure **8-1S** in this work), and $Fe_3(B_3F_3)(CO)_7(\eta^2\text{-}\mu\text{-}CO)$ (structure **8-4S** in this work). For isolated BF ligands the natural charges on both the boron and fluorine atoms are rather insensitive to whether the BF ligand is terminal as in $Fe(BF)(CO)_4$, edge-bridging, or face-bridging. However, the central boron atom in the B_3F_3 chain in structure **8-4S** has a significantly lower positive charge of 0.86 as compared with 1.17 for the other two boron atoms in **8-4S**.

The natural charges on the iron atoms in these fluoroborylene derivatives become more negative as the numbers of their BF groups increase, provided that the bridging BF groups are divided between the iron atoms being bridged (Table 3). However, this analysis is necessarily crude since it is not clear how much of the face-semibridging BF group in **8-1S** to allocate to the iron atom that is further away from it than the other two iron atoms.

The presence of a four-electron donor η^2-μ-CO group is seen to have a major effect on the atomic charge of the iron atom within bonding distance of the oxygen atom. Thus, in structure **8-4S** the iron atom (Fe3) within bonding distance of the oxygen atom of the four-electron donor bridging η^2-μ-CO group is seen to have an unusually low negative charge of −1.21 as compared with the −1.91 negative charge of the iron atom (Fe2) bonded to the carbon atom of the same bridging carbonyl group (Table 3). This indicates the ability of the rather electronegative oxygen atom in the η^2-μ-CO group to withdraw electron density from the iron atom to which it is bonded.

Table 4 lists the Wiberg bond indices (WBIs) for the trinuclear fluoroborylene derivatives $Fe_3(\mu_3\text{-}BF)_2(\mu\text{-}BF)(CO)_9$ (**9-1S**),[14] $Fe_3(\mu_3\text{-}BF)_2(\mu\text{-}BF)(CO)_7(\mu\text{-}CO)$ (**8-1S** in Fig. 3), and $Fe_3(B_3F_3)(CO)_7(\eta^2\text{-}\mu\text{-}CO)$ (**8-4S** in Fig. 3). In **9-1S** all of the Fe–Fe bonds are formal single bonds and their WBIs fall in the narrow range 0.32 ± 0.02, where the WBI of the Fe2–Fe3 bond bridged by the additional μ-BF group is 0.30 and the other two WBIs are 0.34. However, for **8-1S** the WBI for the short Fe1═Fe2 edge of 0.67 is approximately twice that of the other WBIs of 0.27. This supports the assignment of the Fe1═Fe2 edge to a formal double bond and the assignments of the Fe1–Fe3 and Fe2–Fe3 edges to formal single bonds in **8-1S** as discussed above. In **8-4S** all of the iron-iron bonds are assumed to be formal single bonds from electron counting. Indeed, two edges of the Fe_3 triangle in **8-4S**, namely Fe1–Fe2 and Fe1–Fe3, have WBIs of 0.27, which are consistent with the WBIs for the Fe–Fe single bonds in **9-1S** and **8-1S**. However, the third Fe2–Fe3 edge of the Fe_3 triangle in **8-4S**, namely the one bridged by the four-electron donor bridging η^2-μ-CO group, has a much higher WBI of ~0.5. The presence of a bridging η^2-μ-CO group increases significantly the apparent bond order of the edge that it bridges.

4. Discussion

The lowest energy structure for $Fe_3(CO)_{11}$ was predicted in a previous DFT study[15] to have two μ_3-CO groups bridging a Fe_3 triangle with three terminal CO groups on each iron atom (Fig. 5). A completely analogous $Fe_3(BF)_3(CO)_8$ structure requires the third BF group to be a terminal BF group. This apparently is not favorable, so the third BF group becomes a bridging BF group in the lowest energy $Fe_3(BF)_3(CO)_8$ structure **8-1S** (by B3LYP), as in the lowest energy $Fe_3(BF)_3(CO)_9$ structure.[14] In fact the lowest energy $Fe_3(BF)_3(CO)_8$ structure can be derived from the lowest energy $Fe_3(BF)_3(CO)_9$ structure[14] by loss of a CO group from the iron atom not connected to the edge bridged by the μ-BF group. However, one of the CO groups on an adjacent iron becomes a bridging CO group to preserve the number of Fe–C bonds in the structure. This leads to a concentration of four bridging groups (two μ_3-BF, one μ-BF, and one μ-CO) meeting at a single iron atom. In order to avoid the resulting bond congestion both face-bridging BF groups move away from the iron atom bearing both edge bridges, so that they become face-semibridging BF groups with longer Fe–B distances to this "overloaded" iron atom.

The formation of face-semibridging BF groups was previously observed in some of the higher energy $Fe_3(BF)_3(CO)_9$ structures.[14] The Fe–B distances to the face- semibridging BF groups in the lowest energy $Fe_3(BF)_3(CO)_n$ (n = 9, 8) structures are reported in Table 5 as the averages of the

Table 3 Atomic charges from the natural population analysis (NPA) for the $Fe_3(BF)_3(CO)_8$ structures **8-1S**, **8-4S** and the $Fe_3(BF)_3(CO)_9$ structure **9-1S** as well as the $Fe(CO)_4(BF)$ structure with C_{2v} symmetry using the B3LYP and BP86 methods

		Fe1	Fe2	Fe3	$B\mu_3$[a]	$B\mu_3$[a,b]	$B\mu_2$[a]	$F\mu_3$[a]	$F\mu_3$[ab]	$F\mu_2$[a]
8-1S	B3LYP	−1.85	−1.79	−2.67	1.36	1.36	1.42	−0.53	−0.53	−0.53
	BP86	−1.84	−1.77	−2.63	1.34	1.34	1.39	−0.49	−0.49	−0.43
8-4S	B3LYP	−2.27	−1.91	−1.22	0.85	1.20	1.18	−0.50	−0.50	−0.50
	BP86	−2.24	−1.91	−1.21	0.87	1.20	1.14	−0.47	−0.47	−0.47
9-1S	B3LYP	−1.90	−2.41	−2.41	1.30	1.19	1.38	−0.54	−0.53	−0.51
	BP86	−1.93	−2.33	−2.33	1.24	1.16	1.33	−0.50	−0.50	−0.48
$Fe(CO)_4(BF)$	B3LYP	−2.52			1.31			−0.50		
	BP86	−2.48			1.29			−0.46		

[a] The subscripts μ_3 and μ_2 are only relevant for **8-1S**, **8-4S** and **9-1S**. [b] For **8-4S**, this subscript is μ_2.

Table 4 Wiberg bond indices (WBIs) from NBO analysis for the Fe–Fe bonds in $Fe_3(\mu_3\text{-}BF)_2(\mu\text{-}BF)(CO)_9$ (**9-1S**), $Fe_3(\mu_3\text{-}BF)_2(\mu\text{-}BF)(CO)_7(\mu\text{-}CO)$ (**8-1S**), and $Fe_3(B_3F_3)(CO)_7(\eta^2\text{-}\mu\text{-}CO)$ (**8-4S**)

		Fe1–Fe2	Fe1–Fe3	Fe2–Fe3
$Fe_3(\mu_3\text{-}BF)_2(\mu\text{-}BF)(CO)_9$ (**9-1S**)	B3LYP	0.34	0.34	0.30
	BP86	0.33	0.33	0.30
$Fe_3(\mu_3\text{-}BF)_2(\mu\text{-}BF)(CO)_7(\mu\text{-}CO)$ (**8-1S**)	B3LYP	0.69	0.27	0.26
	BP86	0.67	0.27	0.27
$Fe_3(B_3F_3)(CO)_7(\eta^2\text{-}\mu\text{-}CO)$ (**8-4S**)	B3LYP	0.28	0.27	0.52
	BP86	0.27	0.27	0.49

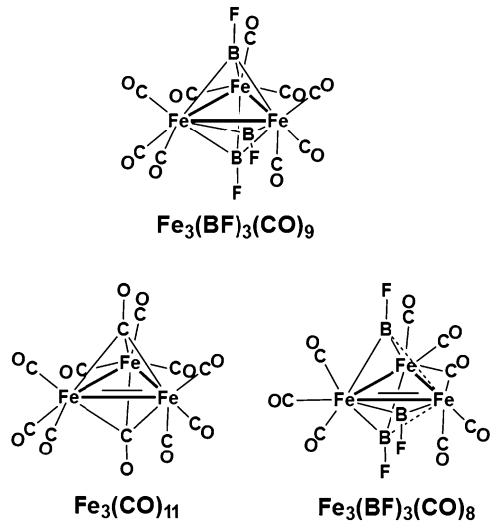

Fig. 5 A comparison of the lowest energy structures for $Fe_3(BF)_3(CO)_9$, $Fe_3(CO)_{11}$, and $Fe_3(BF)_3(CO)_8$.

distances determined by the B3LYP and BP86 methods. The Fe–B distances to the face-bridging μ_3-BF groups in the lowest energy $Fe_3(BF)_3(CO)_9$ structure (**9-1S**) and the lowest energy (by BP86) singlet $Fe_3(BF)_3(CO)_8$ structure **8-1S** (Fig. 4 and Table 1) are given for comparison. The three Fe–B distances to each μ_3-BF group in **9-1S** and **8-1S** are not equivalent because of the asymmetry arising from the single μ-BF bridge of one of the three edges of the Fe_3 triangle. However, the differences between the Fe–B distances in **9-1S** and **8-1S** to the μ_3-BF group, considered as an essentially symmetrical bridge, are much less than those for the Fe–B distances to the face-semibridging groups in the other structures. For the long Fe–B bond distances the variation between the predictions of the two methods is noted. In some cases this is quite large, since these long distances represent relatively weak direct Fe–B interactions.

This study also led to a new type of metal carbonyl fluoroborane structure in which the three BF units have coupled to form a single B_3F_3 unit with B–B distances of $\sim$1.9 Å. Examples of such $Fe_3(BF)_3(CO)_8$ structures are the singlet **8-4S** (Fig. 3 and Table 1), lying only $\sim$7 kcal/mol above the lowest energy singlet structure **8-1S**, and the triplet **8-8T** (Fig. 4 and Table 1) lying at considerably higher energies. These structures may be interpreted in the same manner as the other structures to give the iron atoms 18- or 17-electron configurations as appropriate for the spin state with all of the CO and BF groups functioning as two-electron donors except for the obvious four-electron donor η^2-μ-CO group in **8-4S**. However, the central Fe_3B_3 unit in **8-4S** and **8-8T** forms a bicapped tetrahedron similar the central Os_6 unit in the long-known[16] $Os_6(CO)_{18}$ (Fig. 6), a compound of historical significance in providing impetus for the development of the Wade-Mingos rules.[48–51] In fact **8-4S** is isoelectronic with $Os_6(CO)_{18}$ after considering the following:

(1) The $Fe_2(CO)_4(\eta^2\text{-}\mu\text{-}CO)$ unit in **8-4S** is isoelectronic with two $Fe(CO)_3$ units since the four-electron donor bridging η^2-μ-CO group corresponds electronically and somewhat sterically to two terminal carbonyl groups.

(2) $Fe(CO)_3$ groups are obviously isovalent with $Os(CO)_3$ groups and serve as donors of two skeletal electrons upon applying the Wade-Mingos rules.[48–51]

(3) The BF units are donors of two skeletal electrons like the BH units in polyhedral boranes as well as $Fe(CO)_3$ and $Os(CO)_3$ groups.

Thus $Fe_3(\mu_3\text{-}BF)_2(\mu\text{-}BF)(CO)_7(\mu\text{-}CO)$ (**8-1S**), like $Os_6(CO)_{18}$, has 12 skeletal electrons. This corresponds formally to the skeletal electron requirement of the central Fe_3B tetrahedron in **8-1S**, based on formal two-center two-electron bonds along each of the six edges of this tetrahedron.

Table 5 Fe–B bond lengths (in Å) for the face bridging and semibridging BF groups found in $Fe_3(BF)_3(CO)_9$ and $Fe_3(BF)_3(CO)_8$ structures (averages of the B3LYP and BP86 values)

Structure	No of μ_3-BF groups	Short Fe–B distances	Long Fe–B distance	Other bridges
$Fe_3(BF)_3(CO)_9$ (**9-1S**)[a]	2	2.06	2.19	μ-BF
$Fe_3(BF)_3(CO)_9$ (**9-2S**)[a]	1	2.02	2.45	μ-BF
$Fe_3(BF)_3(CO)_8$ (**8-1S**)	2	2.01	2.33	μ-BF + μ-CO
$Fe_3(BF)_3(CO)_8$ (**8-2S**)	2	1.99	2.50	μ-BF + 2 μ-CO
$Fe_3(BF)_3(CO)_8$ (**8-3S**)	2	1.98	2.49	μ-BF + semi-μ-CO
$Fe_3(BF)_3(CO)_8$ (**8-1T**)	2	2.04	2.23 ± 0.03	μ-BF + 2semi-μ-CO
$Fe_3(BF)_3(CO)_8$ (**8-2T**)	2	2.00 ± 0.04	2.48	semi-μ-CO

[a] The $Fe_3(BF)_3(CO)_9$ structures are designated as in ref. 14. Structure **9-1S** is the lowest energy $Fe_3(BF)_3(CO)_9$ structure by $\sim$19 kcal/mol below **9-2S**.

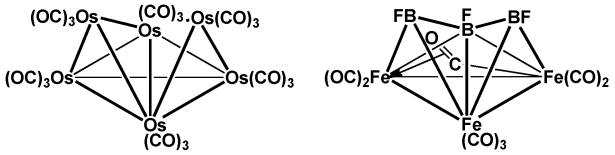

$Os_6(CO)_{18}$ $Fe_3(CO)_7B_3F_3(\eta^2\text{-}\mu\text{-CO})$ (8-4S)

Fig. 6 The related bicapped tetrahedral structures for $Os_6(CO)_{18}$ and $Fe_3(CO)_7B_3F_3(\eta^2\text{-}\mu\text{-CO})$.

5. Summary

This theoretical study of $Fe_3(BF)_3(CO)_8$ structures demonstrates that terminal BF groups are unfavorable relative to bridging BF groups of various types. Thus none of the 15 $Fe_3(BF)_3(CO)_8$ structures within 30 kcal/mol of the global minimum is predicted to have even a single terminal BF group. Instead, in the lowest energy singlet and triplet $Fe_3(BF)_3(CO)_8$ structures two of the three BF groups are μ_3-BF groups bridging the entire Fe_3 triangle whereas the third BF group is a μ-BF group bridging an Fe–Fe edge of the triangle. In most of the low energy $Fe_3(BF)_3(CO)_8$ structures the two μ_3-BF groups are face-semibridging groups with two short Fe–B distances around 2.0 Å and a third significantly longer Fe–B distance around 2.4 Å.

A singlet $Fe_3(B_3F_3)(CO)_7(\eta^2\text{-}\mu\text{-CO})$ structure was also found in which the three BF units form a B_3F_3 unit with B–B distances around 1.9 Å. The central Fe_3B_3 unit in this structure forms a bicapped tetrahedron similar to the central Os_6 unit in $Os_6(CO)_{18}$. This unusual structure lies only ~7 kcal/mol above the lowest energy singlet $Fe_3(BF)_3(CO)_8$ structure and thus suggests the potential accessibility of fluoroborane metal carbonyl clusters having deltahedral structures related to those found in the deltahedral boranes.

Acknowledgements

We are indebted to the 111 Project (B07012) in China, the National Natural Science Foundation of China (Grant 20873045) and the U. S. National Science Foundation (Grants CHE-0749868 and CHE-0716718) for support of this research.

References

1 F. A. Cotton, G. Wilkinson, C. A. Murillo and M. Bochmann, *Advanced Inorganic Chemistry*, Wiley, 6th edn, 1999.
2 P. L. Timms, *J. Am. Chem. Soc.*, 1967, **89**, 1629.
3 P. L. Timms, *Acc. Chem. Res.*, 1973, **6**, 118.
4 K. Kämpfer, H. Nöth, W. Petz and G. Schmid, *Proceedings of the First International Symposium on New Aspects of the Chemistry of Metal Carbonyl Derivatives*, Inorganica Chimica Acta, Padova, Italy, 1968.
5 D. Vidović and S. Aldridge, *Angew. Chem., Int. Ed.*, 2009, **48**, 3669.
6 X. Wang, B. O. Roos and L. Andrews, *Angew. Chem. Int. Ed.*, 2010, **49**, 157.
7 X. Wang, B. O. Roos and L. Andrews, *Chem. Commun.*, 2010, **46**, 1646.
8 G. J. Irvine, M. J. G. Lesley, T. B. Marder, N. C. Norman, C. R. Rice, E. G. Robins, W. R. Roper, G. R. Whittell and L. J. Wright, *Chem. Rev.*, 1998, **98**, 2685.
9 H. Braunschweig, R. D. Dewhurst and A. Schneider, *Chem. Rev.*, 2010, **110**, 3924.
10 R. Okamura, K. Tada, K. Matsubara, M. Oshims and H. Suzuki, *Organometallics*, 2001, **20**, 4772.
11 H. Braunschweig, C. Burschka, M. Burzler, S. Metz and K. Radacki, *Angew. Chem., Int. Ed.*, 2006, **45**, 4352.
12 H. Braunschweig and M. Mueller, *Chem. Ber.*, 1997, **130**, 1295.
13 L. Xu, Q.-S. Li, Y. Xie, R. B. King and H. F. Schaefer, *Inorg. Chem.*, 2010, **49**, 1046.
14 L. Xu, Q.-S. Li, Y. Xie, R. B. King and H. F. Schaefer, *Inorg. Chem.*, 2010, **49**, 2996.
15 H. Wang, Y. Xie, R. B. King and H. F. Schaefer, *J. Am. Chem. Soc.*, 2006, **128**, 11376.
16 R. Mason, K. M. Thomas and D. M. P. Mingos, *J. Am. Chem. Soc.*, 1973, **95**, 3802.
17 A. W. Ehlers and G. Frenking, *J. Am. Chem. Soc.*, 1994, **116**, 1514.
18 B. Delley, M. Wrinn and H. P. Lüthi, *J. Chem. Phys.*, 1994, **100**, 5785.
19 J. Li, G. Schreckenbach and T. Ziegler, *J. Am. Chem. Soc.*, 1995, **117**, 486.
20 V. Jonas and W. Thiel, *J. Chem. Phys.*, 1995, **102**, 8474.
21 T. A. Barckholtz and B. E. Bursten, *J. Am. Chem. Soc.*, 1998, **120**, 1926.
22 S. Niu and M. B. Hall, *Chem. Rev.*, 2000, **100**, 353.
23 P. Macchi and A. Sironi, *Coord. Chem. Rev.*, 2003, **238–239**, 383.
24 M. Buhl and H. Kabrede, *J. Chem. Theory Comput.*, 2006, **2**, 1282.
25 P. Morschel, J. Janikowski, G. Hilt and G. Frenking, *J. Am. Chem. Soc.*, 2008, **130**, 8952.
26 T. Ziegler and J. Autschbach, *Chem. Rev.*, 2005, **105**, 2695.
27 M. P. Waller, M. Bühl, K. R. Geethanakshmi, D. Wang and W. Thiel, *Chem.–Eur. J.*, 2007, **13**, 4723.
28 P. G. Hayes, C. Beddie, M. B. Hall, R. Waterman and T. D. Tilley, *J. Am. Chem. Soc.*, 2006, **128**, 428.
29 M. Bühl, C. Reimann, D. A. Pantazis, T. Bredow and F. Neese, *J. Chem. Theory Comput.*, 2008, **4**, 1449.
30 M. Besora, J.-L. Carreon-Macedo, J. Cowan, M. W. George, J. N. Harvey, P. Portius, K. L. Ronayne, X.-Z. Sun and M. Towrie, *J. Am. Chem. Soc.*, 2009, **131**, 3583.
31 S. Ye, T. Tuttle, E. Bill, L. Simkhorich, Z. Gross, W. Thiel and F. Neese, *Chem.–Eur. J.*, 2008, **14**, 10839.
32 A. D. Becke, *J. Chem. Phys.*, 1993, **98**, 5648.
33 C. Lee, W. Yang and R. G. Parr, *Phys. Rev. B: Condens. Matter*, 1988, **37**, 785.
34 A. D. Becke, *Phys. Rev. A: At., Mol., Opt. Phys.*, 1988, **38**, 3098.
35 J. P. Perdew, *Phys. Rev. B: Condens. Matter*, 1986, **33**, 8822.
36 See especially F. Furche and J. P. Perdew, *J. Chem. Phys.*, 2006, **124**, 044103.
37 H. Y. Wang, Y. Xie, R. B. King and H. F. Schaefer, *J. Am. Chem. Soc.*, 2005, **127**, 11646.
38 I. Silaghi-Dumitrescu, T. E. Bitterwolf and R. B. King, *J. Am. Chem. Soc.*, 2006, **128**, 5342.
39 T. H. Dunning, *J. Chem. Phys.*, 1970, **53**, 2823.
40 T. H. Dunning and P. J. Hay, *Methods of Electronic Structure Theory*, ed. H. F. Schaefer, Plenum, New York, 1977, pp. 1–27.
41 S. Huzinaga, *J. Chem. Phys.*, 1965, **42**, 1293.
42 A. J. H. Wachters, *J. Chem. Phys.*, 1970, **52**, 1033.
43 D. M. Hood, R. M. Pitzer and H. F. Schaefer, *J. Chem. Phys.*, 1979, **71**, 705.
44 M. J. Frisch, *et al.*, *GAUSSIAN 03, Revision C 02*, Gaussian, Inc., Wallingford CT, 2004 (see Supporting Information for details).
45 M. Reiher, O. Salomon and B. A. Hess, *Theor. Chem. Acc.*, 2001, **107**, 48.
46 F. A. Cotton and J. M. Troup, *J. Am. Chem. Soc.*, 1974, **96**, 4155.
47 F. Weinhold and C. R. Landis, *Valency and Bonding: A Natural Bond Order Donor–Acceptor Perspective*, Cambridge University Press, Cambridge, England, UK, 2005.
48 K. Wade, *Chem. Comm.*, 1971, 792.
49 K. Wade, *Adv. Inorg. Chem. Radiochem.*, 1976, **18**, 1.
50 D. M. P. Mingos, *Nature Phys. Sci.*, 1972, **99**, 236.
51 D. M. P. Mingos, *Acc. Chem. Res.*, 1984, **17**, 311.